Journal of the Chinese Chemical Society, **1997**, *44*, 337-348

Structural Characterization of Venom Toxins by Physical Methods and the Perspectives on Structure-Function Correlation of Proteins

Shyh-Horng Chiou (邱式鴻) and Shih-Hsiung Wu (吳世雄)
Institute of Biochemical Sciences, National Taiwan University and Institute of Biological Chemistry, Academia Sinica, P.O. Box 23-106, Taipei, Taiwan, R.O.C.

This account describes work in our laboratories on the application of physical methods to the structural studies of various toxins during the past few years. A general review of background and the meaningful results obtained from these approaches are described. The results are compared with updated information on related subjects carried out at other laboratories. Examples of structural studies on some small toxins present abundantly in Formosan cobra (*Naja naja atra*), one of the indigenous toxic snakes in Taiwan, are given with the emphasis on the identification and characterization of complex toxic protein components based on near-infrared Fourier transform Raman Spectroscopy. We will also describe our initial efforts in solving the solution structures of several small proteins and peptides by means of two-dimensional nuclear magnetic resonance (2D-NMR) and computer-simulated modeling. The structural information obtained by these modern physical techniques provides the framework for unraveling the complex structure-activity relationships engendered by these biomolecules.

INTRODUCTION

Venom research has a long and distinctive history in the basic medical research of Taiwan. Most notable are the extensive studies done chemically and pharmacologically on the venom toxins of the elapid snakes during the past four decades.[1,2] The components isolated from crude venoms of the most poisonous **Elapidae** family generally fall into three major categories based on their structures and activities, *i.e.* (A) phospholipases A_2 (B) neurotoxins and (C) cardiotoxins (or called cytotoxins). All these biologically active proteins have been used widely as tools in the studies of various biological phenomena of molecular and cell biology.

Traditionally protein purification occupied a central position in many areas of biochemical research. With the recent advances in gene cloning and expression it becomes even more obvious that the efficient method of obtaining pure protein samples is always a prerequisite for meaningful structure-function studies. Currently, most toxin components of snake venoms can be obtained in relatively pure forms from crude venoms by simple ion-exchange chromatography coupled with gel permeation and/or high-performance liquid chromatography (HPLC). In the initial stage of embarking on a structural characterization of biomolecules, it is important to find a non-invasive and sensitive technique for preliminary structural studies before a detailed structure-activity correlation can be pursued. In this regard Nuclear Magnetic Resonance (NMR) and Raman Spectroscopy have rapidly become two useful physical methods of choice for biological samples.

The main advantage of the Raman technique lies in its potential to study biological samples such as nucleic acids and proteins both in the solid and solution states.[3-5] The recent advance of Fourier transform Raman technique (FT-Raman) is especially attractive since it circumvents the requirement of very high sample concentration used for the conventional Raman spectroscopy. In this report we apply the new near-IR FT-Raman spectroscopy to the studies of purified phospholipase A_2 (PLA_2), neurotoxin (cobrotoxin) and several cardiotoxin analogues isolated from the Taiwan cobra, *Naja naja atra*.

NMR and X-ray diffraction are the two pre-eminent techniques of current active research in the realm of structural biology.[6,7] Although they have been used independently and successfully for the structure determination of more than several hundred proteins or peptides (Protein Data Bank, about 900 unique structures not derivatives or site-specific mutants have been deposited during 1985-95), some limitations and advantages/disadvantages are intrinsically associated with each technique. NMR is well known to be the method of choice in the study of protein structure in solution; in contrast X-ray diffraction study is limited to the solid or crystal structure of proteins. Moreover, conformational flexibility or the dynamics of protein structures are usually involved in biomolecular recognition, *e.g.* ligand-receptor interaction, which is only amenable to NMR solu-

Dedicated to Professor Yu-Shia Cheng on the occasion of her 65th birthday.

tion study, but not suitable for X-ray study. In this regard, NMR has become popular of late as a unique and major tool in the study of correlation between dynamics and function of biomolecular structures. Herein, we report our initial successful application of high-resolution NMR to the studies of solution structures for two venom toxic peptides with profound biological activity.

RESULTS AND DISCUSSION

Isolation and Characterization of Venom Toxins from Taiwan Cobra

Fig. 1 shows the general elution pattern of the crude venom from Taiwan cobra on TSK CM-650 cation-exchange column. The well-defined separation of venom components on the preparative column was corroborated by the pharmacological assays similar to that reported previously on the venom separation from the other closely-related species *Naja naja siamensis*.[8] It is shown that C2 and C4 fractions contain PLA_2 activity whereas C4, C6-C8 belong to neurotoxin and cardiotoxin, respectively. The relative yield percents for each toxin fraction are about 20%, 8-10%, and 40% for PLA_2, neurotoxin (or cobrotoxin), and cardiotoxin, respectively. C5 fraction, which possessed strong PLA_2 activity, is found to be slightly contaminated with C4 of cobrotoxin[9] when it was analyzed by reversed-phase HPLC. It needs to be passed through a second chromatographic step before amino acid analysis and FT-Raman study. C6, C7, and C8 fractions, which represent about 40% of total crude proteins, belong to the cardiotoxin (or termed cytotoxin) class based on pharmacological and N-terminal sequence analysis (data not shown). Since these three toxins are major toxin components and constitute more than half of the total proteins in the venom, they have been used for FT-Raman study shown below.

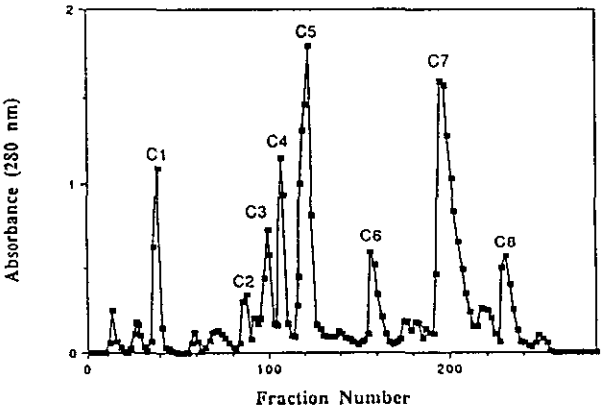

Fig. 1. Cation-exchange chromatography on TSK CM-650(S) column of crude venom from Formosan cobra, *Naja naja atra*. About 500 mg of lyophilized crude venom dissolved in the starting buffer of 0.05 M ammonium acetate, pH 5.7, was applied to the column equilibrated with the same buffer. Elution was carried out in four steps: (A) elution with starting buffer (Fractions 1-40); (B) elution with a linear gradient of 0.1-0.5 M ammonium acetate, pH 5.9 (Fractions 41-140); (C) a linear gradient of 0.7-1.0 M ammonium acetate, pH 5.9 (Fractions 141-200) and (D) 1.0 M ammonium acetate, pH 5.9 (Fractions 201-280). The column eluates (6.3 mL/tube per 5.5 min) were monitored for absorbance at 280 nm. The peak fractions were collected, lyophilized and used for pharmacological assays and FT-Raman studies. Fraction C5 was shown to be contaminated with C4 and repurified on reversed-phase HPLC before spectroscopic analysis.

FT-Raman Spectroscopic Study on the Purified PLA_2 and Toxins of Cobra Venom

Relatively fewer studies have been done on the structural and conformational study of venom toxins using laser Raman techniques as compared to other types of approaches such as sequence analysis coupled with circular dichroism (CD) and X-ray diffraction. Previous Raman studies were limited by the concentration requirement for solution study (> 50 mg/mL) and the strong fluorescent background of Raman spectra both in solution and solid states. However with the advance in the instrumentation important information about peptide backbone, geometry of disulfide bonds and the microenvironments of aromatic amino acids and methionine plus the presence of sulfhydryl groups in the native proteins [3-5 and references cited therein] are still obtained using conventional Raman spectrophotometers. Raman techniques overcome the disadvantages of CD and fluorescence in obtaining the structural information in the solid state and complement X-ray diffraction in gaining structural insight into proteins in aqueous solution. Now, taking advantage of incorporating Fourier transform technique into Raman spectrophotometer, near-IR FT-Raman similar to the well-established FT-IR enables the elimination of water background and fluorescent interference associated with the use of a conventional visible laser as the excitation source. Using this new instrumentation, we have reported the first FT-Raman spectra on the purified toxin components.[10,11]

Comparison of FT-Raman Spectra of Cobrotoxin, Cardiotoxin, and PLA_2

Cobrotoxin (C4) is the most toxic non-enzyme princi-

ple found in Formosan cobra venom.[12] It is a small polypeptide chain of 62 amino acids cross-linked by 4 disulfide bonds.[9,13] Previous CD[14] and Raman[15] studies have indicated a predominance of β-pleated sheet structure in this small toxin, which is also in accord with the results of X-ray crystal structures of some neurotoxins from sea-snake venoms.[16,17]

The near-IR FT-Raman spectra for purified cobrotoxin (C4), PLA_2 (C5), and cardiotoxin (C7) are shown in Fig. 2, Fig. 3, and Fig. 4, respectively for comparison. Since the previous pilot laser-Raman study of snake toxins[3,4] has indicated almost identical Raman spectra for the lyophilized solid and aqueous samples, only the FT-Raman spectra of lyophilized powders are shown in this comparative study.

It is noteworthy that defined and clear-cut features of FT-Raman spectra with low fluorescence interference are easily obtained as compared to the conventional Raman study with high-noise background and non-linear baseline in most of the reported Raman spectra.[15,18-20] Moreover the sample requirement in this study is only 1-2 mg, much lower than that used in the conventional Raman study (50-100 mg/mL for solution study and about 5-10 mg for solid samples). The assignments of well-defined Raman peaks obtained from the new FT-Raman spectra for these toxins and their comparison and discrepancies with some of reports in the literature are discussed below.

Characteristic peak assignments for cobrotoxin

In Fig. 2 the amide I band at 1671 cm^{-1} is clearly indicative of an anti-parallel β-sheet structure when compared to the model β-sheet structures of poly-L-valine[21] or denatured insulin.[22] The amide III band at 1238-1248 cm^{-1} for cobrotoxin also indicated that cobrotoxin did not possess appreciable amounts of α-helical content since the α-helix conformation usually gave this band above 1260 cm^{-1}.[23] Therefore from the amide I and III bands it is concluded that cobrotoxin consists mainly of a β-sheet structure, which is also consistent with the CD study of the same toxin.[24] It is of note that this neurotoxin lacks a vibration band at 1004 cm^{-1}, which is related to the breathing vibration of the mono-substituted phenylalanine (Phe) ring.[3-5] Amino acid composition shown in Table 1 corroborates this observation in indicating no Phe residues detected in cobrotoxin. The inten-

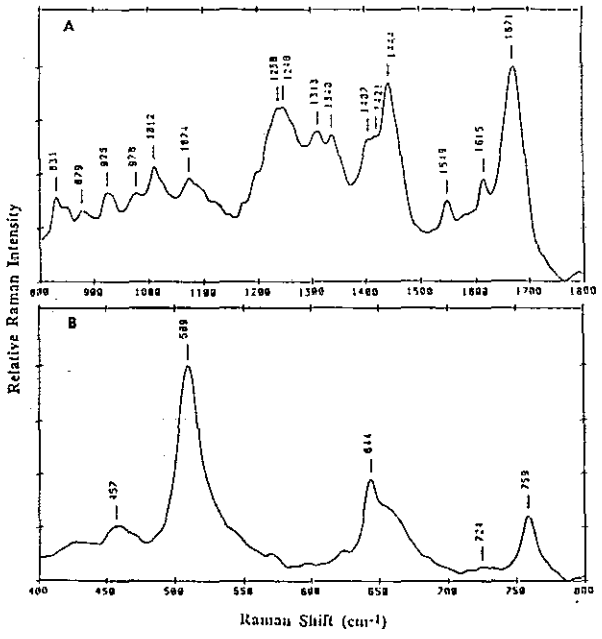

Fig. 2. Raman spectra of lyophilized cobrotoxin in the (A) 800-1800 cm^{-1} and (B) 400-800 cm^{-1} frequency region. Cobrotoxin corresponds to the C_4 fraction in Fig. 1. Sample preparation is described in Materials and Methods. Data collection was carried out under the following conditions: excitation wavelength, 1.064 mm; laser power, 180 mW; spectral resolution, 4 cm^{-1}; total scans, 2000 (108 min). Major vibration band frequencies in cm^{-1} are labelled on the spectra.

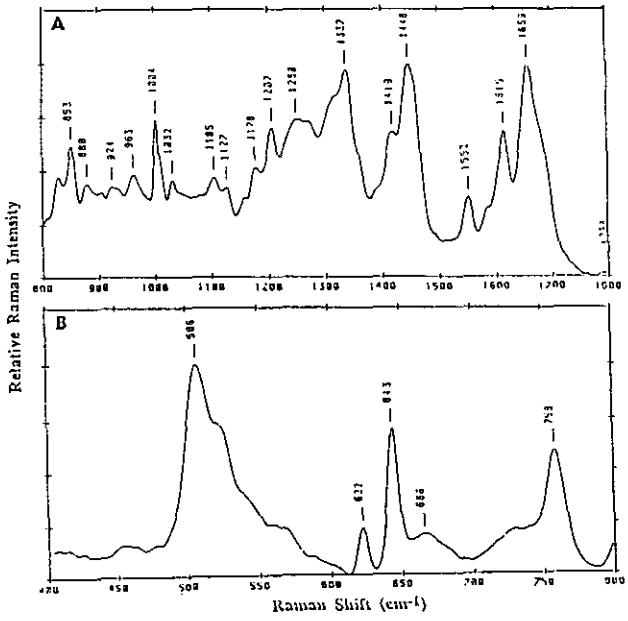

Fig. 3. Raman spectra of lyophilized phospholipase A_2 in the (A) 800-1800 cm^{-1} and (B) 400-800 cm^{-1} frequency region. Phospholipase A_2 (PLA_2) corresponds to the C_5 fraction in Fig. 1. Sample preparation is described in Materials and Methods. Data collection was carried out under the following conditions: excitation wavelength, 1.064 mm; laser power, 180 mW; spectral resolution, 4 cm^{-1}; total scans, 2000 (108 min). Major vibration band frequencies in cm^{-1} are labelled on the spectra.

sity ratio of tyrosine (Tyr) lines at 831/853 cm^{-1} pointed to the fact that 2 tyrosines in the toxin are probably buried instead of being exposed on the surface.[3] The bands at 759, 879, and 1012 cm^{-1} reflected the single tryptophan (Trp) ring vibration present in this molecule. The lack of a Trp C-H deformation band at about 1360 cm^{-1} is diagnostic of a relatively exposed microenvironment for this Trp residue. The missing bands located at 724 and 622 cm^{-1} in turn reflected the absence of methionine (Met) and Phe, respectively. The strong and symmetrical stretching vibration band at 509 cm^{-1} can be assigned to a uniform and similar geometry about the internal rotation of C-S bonds present in the 4 disulfide bonds in this compact toxin. They could probably be assigned as a gauche-gauche-gauche type conformation as suggested by the study using model compounds.[25,26] We could not detect the vibration frequency of sulfhydryl groups in the 2550-2600 cm^{-1} region for the crude venom on any of the three purified toxin components (data not shown), which is consistent with the sulfhydryl/disulfide status in secretory proteins such as venom toxins. In general FT-Raman spectra on these toxins give a better correlation to the exact structural data such as amino acid composition for these toxins than that obtained by the conventional Raman technique.

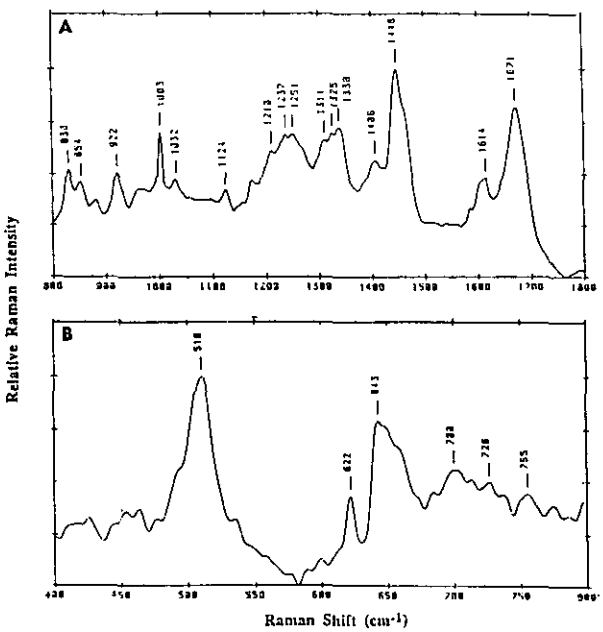

Fig. 4. Raman spectra of lyophilized cardiotoxin in the (A) 800-1800 cm^{-1} and (B) 400-800 cm^{-1} frequency region. Cardiotoxin corresponds to the C_7 fraction in Fig. 1. Sample preparation is described in Materials and Methods. Data collection was carried out under the following conditions: excitation wavelength, 1.064 mm; laser power, 180 mW; spectral resolution, 4 cm^{-1}; total scans, 2000 (108 min). Major vibration band frequencies in cm^{-1} are labelled on the spectra.

Table 1. Amino Acid Compositions of Cobrotoxin, Phospholipase A_2 and Cardiotoxin

Amino acids	Cobrotoxin (C_4)	Phospholipase A_2 (C_5)	Cardiotoxin (C_7)
1/2Cys	7.5 (8)	13.4 (14)	7.8 (8)
Asx	7.7 (8)	21.2 (21)	5.7 (6)
Thr	7.7 (8)	4.4 (5)	2.7 (3)
Ser	3.5 (4)	4.3 (5)	1.5 (2)
Glx	6.6 (7)	7.9 (8)	0.3 (0)
Pro	1.7 (2)	3.9 (4)	4.6 (5)
Gly	6.8 (7)	8.8 (9)	1.8 (2)
Ala	0.2 (0)	11	2
Val	0.7 (1)	3.7 (4)	6.8 (7)
Met	0.3 (0)	0.7 (1)	1.8 (2)
Ile	1.7 (2)	4.1 (4)	0.7 (1)
Leu	1	4.8 (5)	5.9 (6)
Tyr	1.7 (2)	8.5 (9)	2.8 (3)
Phe	0.2 (0)	3.7 (4)	1.6 (2)
His	1.8 (2)	0.8 (1)	0.2 (0)
Lys	2.8 (3)	4.8 (5)	8.8 (9)
Arg	5.6 (6)	5.7 (6)	1.8 (2)
Trp	0.8 (1)	2.8 (3)	0.1 (0)
Total residues	(62)	(119)	(60)

Fractions C_4, C_5, and C_7 correspond to the lyophilized fractions labeled in Fig. 1. Data are expressed as the number of residues per molecule of protein using leucine or alanine as the references to calculate the residues of other amino acids. Values represent the mean of duplicate determinations. The hydrolysis condition is microwave irradiation for 5 min using 6 M HCl or 4 M methanesulfonic acid containing 0.2% 3-(2-aminoethyl)indole. Values in the parentheses show the theoretical number of amino acid residues calculated from the published sequences. Note that the compositions of C_6 and C_8 are almost identical to C_7.

Characteristic peak assignments for PLA_2

PLA_2 is an enzyme widely distributed among various species in the animal kingdom, notably in the pancreatic tissues of mammals and in the venoms of snakes and bees. While it is present as a single-chain enzyme in most snake venom, it can also form a toxic complex with a small neurotoxin in the venoms of some South American rattlesnakes.[27] In our purification of Formosan cobra venom we consistently found the contamination of PLA_2 (C5) by cobrotoxin (C4), which can be removed by one more step of gel-permeation chromatography or reversed-phase HPLC. Previous pharmacological studies of neurotoxins or cardiotoxins of snake venom were sometimes complicated by the unexplained PLA_2-like activity [1,2 and references cited therein]. We believe that a preliminary FT-Raman spectra check of the studied toxins would help evaluate the purities

of various samples suspected of contamination. As shown in Fig. 3 for the purified PLA_2, the amide I band at 1659 cm^{-1} is certainly distinguished from that of cobrotoxin (Fig. 2) at 1671 cm^{-1}. The presence of sharp stretching bands at 1004 and 622 cm^{-1}, in contrast to the absence of these bands in cobrotoxin, would attest to the existence of Phe residues in PLA_2 (Table 1). The well-defined Tyr doublet at 853/831 cm^{-1} with a ratio of greater 1 suggested that most of 9 Tyr residues are exposed or in a hydrophilic microenvironment. The shoulder bands at 724 and 666 cm^{-1} associated with the vibration modes of C-S bonds could be ascribed to the single methionine in PLA_2. The presence of Trp stretching bands at 758 and 880 cm^{-1} and not found at 1360 cm^{-1} would also indicate a less rigid environment for the 3 Trp residues in PLA_2. There are several shoulder peaks in addition to the sharp strong disulfide stretching peak at 506 cm^{-1} which are different from the symmetrical band of 509 cm^{-1} present in cobrotoxin. The C-S-S-C stretching modes of the seven disulfide bonds are probably not quite as uniform as those shown in the gauche-gauche-gauche conformation of cobrotoxin. It is worth noting that there is so far only one vibration study on PLA_2 isolated from the South American rattlesnake *Crotalus durissus terrificus*[20] The Raman spectra of this report did not show well-resolved vibration bands for amide I and III, which led to the conclusion that conformational changes occur for PLA_2 molecules as a consequence of different physical states and that different secondary-structure contents were estimated under different experimental conditions. In contrast to this report we found different PLA_2 of the same Elapidae family showed essentially similar α-helical conformations of the peptide backbone with only small contributions from random coil or β-sheet conformations (unpublished results). The structural differences detected by FT-Raman in these PLA_2 involved mainly the microenvironments of aromatic amino acids. The recent crystal structure study and comparison of PLA_2 from the venom of Formosan cobra and bee venom seemed to indicate a conservation of the structural elements even from these two divergent sources.[28,29] A structural comparison of PLA_2 from different snake families and insects employing FT-Raman is currently under study.

Comparison of FT-Raman spectra of cardiotoxin (C7) and cobrotoxin (C4)

Cardiotoxins are a group of very basic polypeptides in some snake venoms, especially abundant in the Elapidae family such as Formosan cobra.[1] They constitute about 40% of total protein in the crude venom. Their functions are more diverse, and their pharmacological modes of action are less well understood than those of the more potent neurotoxins such as cobrotoxin. The primary sequences of several closely-related cardiotoxins from the Formosan cobra are known and shown to be partially related to neurotoxins. They possess distinct pharmacological and biochemical properties despite the existence of a grossly similar tertiary structure among these toxins, *i.e.* a core consisting of a series of short loops and four disulfide bridges. There are in general no specific non-invasive physical methods to distinguish between neurotoxins and cardiotoxins. However FT-Raman spectra of cobrotoxin (Fig. 2) and cardiotoxin (Fig. 4) show some defined structural differences which can be correlated with their amino acid compositions.

All cardiotoxin isoforms (C6, C7 and C8) showed similar stretching amide I and III bands at 1671-1672 and 1235-1250 cm^{-1}, respectively, indicative of a β-sheet secondary structure. In contrast to cobrotoxin they exhibited a sharp band at 1003 cm^{-1} corresponding to the presence of 2 Phe residues in cardiotoxin. The ratio of Tyr doublet at 854/830 cm^{-1} suggested that Tyr residues are probably buried, similar to that in cobrotoxin. The intensity ratio at 622/644 cm^{-1} would indicate a higher content of Tyr than Phe, which is also consistent with the result of amino acid analysis (Table 1). The stretching bands at 654 and 725 cm^{-1} are reflective of the existence of Met residues in these cardiotoxins. The disulfide stretching band at 510 cm^{-1} pointed to a gauche-gauche-gauche conformation for the internal rotation of C-S-S-C bonds. The spectra of three isotoxins (C6, C7 and C8) are closely similar to each other with only minor intensity change in some of the overlapping stretching bands. This is corroborated by the amino acid analysis, which indicated almost identical composition among these three fractions (unpublished results). A summary of the characteristic vibration bands present in cobrotoxin and three major isoforms of cardiotoxins is tabulated in Table 2.

In conclusion a systematic study of the purified venom toxins by the newer FT-Raman spectroscopy is carried out to provide a non-invasive physical method in establishing the structural differences among these biologically active polypeptides. Higher quality spectra with good correlation to the structural data than the conventional Raman spectroscopy could be obtained using near-IR FT-Raman in a relatively short time. It should prove valuable in the clarification and structural characterization of new toxin components from various venoms.

Structure Analysis of Echistatin Analogues by NMR and Computer Graphics

Several polypeptides isolated from snake venoms such as trigramin[30,31] and echistatin[32-34] have been shown to possess inhibitory effects on platelet aggregation.[35] These

Table 2. Characteristic Raman Bands of Cobrotoxin and Cardiotoxins

Raman shift (cm^{-1}) assignments	Cobrotoxin (C_4)	Cardiotoxins (C_6,C_7,C_8)
Amide I	1671	1671-1672
Amide III	1238-1248	1237-1251
Tyr doublet		
Fermi resonance	831/853 > 1	830/854 > 1
Phe		
Aromatic ring vibration	none	1003
Phe/Tyr ratio	622/644 ~ 0	622/644 < 1
Trp		
Indole ring vibration	759,879	none
Met		
C-S stretching vibration	none	701,724
Disulfide		
S-S stretching vibration	509	510,540

The Raman vibration bands correspond to those shown in Figs. 2-4. Note that Raman spectra correlate with the structural data from amino acid compositions shown in Table 1.

polypeptides can block aggregation through interference with fibrinogen binding to their specific receptors on the platelet surface membrane in a competitive manner and are designated as the "disintegrin" family of venom peptides. Among disintegrins, echistatins are the smallest members of this family of polypeptides with regard to their molecular sizes. Four different echistatins, designated as echistatin α1, α2, β and γ,[32-34] were isolated and their amino acid sequences were determined. The exact spatial linkage of disulfide bridges (Cys2-Cys11, Cys7-Cys32, Cys8-Cys37 and Cys20-Cys39) in echistatin α1, which was first predicted by a statistical analysis of the NMR-deduced structures.[36] The three-dimensional structure of echistatin α_1 in solution, which was generated by NMR and computer modeling, showed that the main recognition site (Arg-Gly-Asp, *i.e.* RGD sequence) is located on an exposed and mobile loop; however, the conformation and orientation of N- and C-terminal residues are poorly defined.[36,37] From the analysis of protein sequences and disulfide-bond locations of various disintegrins, a domain containing the RGD sequence appears to be conserved and confined within two pairs of disulfide bonds. On the other hand, the disulfide bond Cys8-Cys37 of echistatins appears not to be conserved when comparing the sequences of echistatins with other larger disintegrins.[37,38] This has prompted us to synthesize an echistatin γ analogue with three disulfide bonds, des(46-49)-[$Ala^{8,37}$]-echistatin γ, which was made by replacing Cys8 and Cys37 residues with alanine. The synthetic analogue was characterized by ion-spray mass spectroscopy, amino acid analysis, and biological assay. Its tertiary structure was further determined by solution NMR spectroscopy and molecular modeling methods.

2D-NMR study of des(46-49)-[$Ala^{8,37}$]-echistatin γ

In order to determine the structure of des(46-49)-[$Ala^{8,37}$]-echistatin γ, we have obtained a complete set of proton 2D-NMR spectra for this synthetic analogue, including "double-quantum filtered correlation spectroscopy" (DQF-COSY), "total correlation spectroscopy" (TOCSY) and "nuclear Overhauser and exchange spectroscopy" (NOESY) (Fig. 5) at different mixing times. Analysis of the amino acid spin systems began with the amide to aliphatic region of TOCSY spectra of des(46-49)-[$Ala^{8,37}$]-echistatin γ in H_2O. The C_α proton resonances were identified by comparison with the fingerprint region of DQF-COSY spectra (H_2O). Five groups of spin systems were initially identified from the TOCSY experiment by inspection of the NH to $C_\alpha H$, $C_\beta H$, $C_\gamma H$ and $C_\delta H$ connections. The five groups were (i) Gly with two C_α proton resonances, (ii) Thr and Ala spin systems, (iii) Ile and Leu spin systems, (iv) AMX spin systems with C_β proton resonance between 2.5 and 4.0 ppm, and (v) Long side chain spin systems (Lys, Arg and Glu) where at least three cross peaks from the side chain to the amide proton were observed. Des(46-49)-[$Ala^{8,37}$]-echistatin γ contains three Pro, three Arg, three Lys, two Met, two Glu, three Asn, one Phe, one Tyr, one His, one Ser, six Cys and six Asp residues. Of these spin systems, the three Pro were identified by observing the complete connectivity pattern between the protons. The spin systems of Arg and Lys were distinguishable and were assigned by the sequential assignment procedure. The aromatic ring protons of Phe, Tyr and His were readily determined by inspection of the spectra in the aromatic region. Using the sequential assignment procedure, specific assignments for the amino acids were obtained based on all ^{1}H-NMR chemical shifts of the synthetic peptide (Table 3). The sequential "nuclear Overhauser effect" (NOE) connectivities d_{NN}, $d_{\alpha N}$, and $d_{\beta N}$, together with other NMR parameters, were used for the complete structural assignments.

Tertiary structure analysis of des(46-49)-[$Ala^{8,37}$]-echistatin γ by computer graphic modeling

We have constructed the superposition of 15 structures of the backbone atoms of the des(46-49)-[$Ala^{8,37}$]-echistatin γ (Fig. 6), selected from 40 structures determined from NOE constraints. The structures are well defined and in good superposition among themselves with proper tertiary folding.

The superposition of the three segments of this synthetic analogue regarding the backbone atoms in the two turn regions and α-carbon presentation in the RGD loop region is also excellent with the average RMS deviation from the mean structure being 0.68 Å for the backbone atoms and 1.15 Å for all atoms. None of the structures have violations of the NOE constraints greater than 0.5 Å, and the deviations from the idealized covalent geometry are small. The nonbonded contacts for these structures are also characterized by a large negative Lennard-Jones van der Waals energy, showing the conversion of different structures into a low energy state of an acceptable conformation by energy minimization.

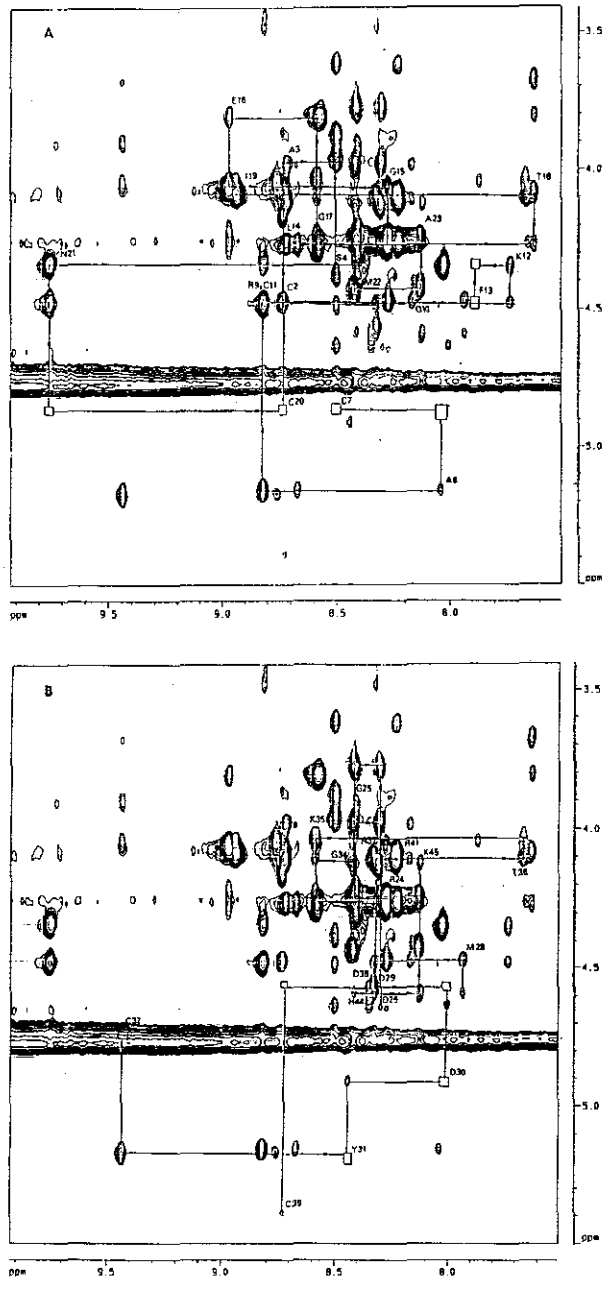

Fig. 5. NOESY spectra of des(46-49)-[Ala^{8,37}]-echistatin γ recorded in 90% H_2O/10% ^2H_2O at 27 °C for a mixing period of 150 ms. The sequential dαN connectivities are shown for the sequence segments (A) residues #1-23, and (B) residues #24-45.

The main differences between the synthetic analogues and the native toxin lie in the C-terminal part due to the deletion of residues #46-49. The replacement of two Cys residues at #8 and #37 with alanine does not appear to change much on the tertiary structure of the native toxin molecule. Therefore, the disulfide pair of Cys^8-Cys^{37} may not play an essential role for the structural organization of the toxin polypeptide, which is strengthened by activity assay. Moreover the C-terminal four residues (#46-49) were shown to have little effect on the biological activity and structure as revealed in our previous study.[39] The present study further demonstrates that the linear sequence of des(46-49)-[Ala^{8,37}]-echistatin γ with three disulfide bonds (Cys^2-Cys^{11}, Cys^7-Cys^{32} and Cys^{20}-Cys^{39}) is sufficient for specifying the biological function and folding pattern.

Protein Engineering of Waglerin I by Synthetic Approach and NMR Dynamic Simulation and Modeling

Waglerin was first isolated from *Trimeresurus wagleri*, a small, toxic arboreal snake distributed from Malaysia, the Philippines, Thailand, and the Indo-Australian archipelago to Indonesia.[40] It is a peptide toxin composed of 22 amino-acid residues with one disulfide bond.[41,42] Most noteworthy is the salient feature of the amino acid composition of waglerin, which contains seven proline residues out of 22 amino acids and a high content of basic amino

Fig. 6. Stereo views of the structure of des(46-49)-[Ala^{8,37}]-echistatin γ calculated by distance geometry and simulated annealing. The backbone atoms of the 15 selected solution structures are superimposed. The missing disulfide bond is replaced by Ala-8 and Ala-37 and marked red in the C_α position. N- and C-terminal ends are marked in blue.

Table 3. ^{1}H-NMR Chemical Shifts of des(46-49)-[Ala^{8,37}]-echistatin γ (H_2O containing 10% D_2O, 27 °C)

Residue	Chemical shift (ppm)					
	NH	$C_\alpha H$	$C_\beta H$	$C_\gamma H$	$C_\delta H$	others
Asp1		4.20	2.73, 2.82			
Cys2	8.74	4.62	3.00, 3.19			
Ala3	8.71	4.02	1.24			
Ser4	8.51	4.42	3.92, 3.98			
Cly5	8.35	4.53, 4.42				
Pro6		4.54	2.57, 1.88	2.18, 2.08	3.64, 3.91	
Cys7	8.51	5.00	2.57, 2.57			
Ala8	8.06	5.20	0.97			
Arg9	8.84	4.53	1.66, 1.67	1.64, 1.52	3.19, 3.29	7.19 ($N_\varepsilon H$)
Asp10	8.15	4.52	2.54, 2.65			
Cys11	8.84	4.53	3.47, 3.52			
Lys12	7.76	4.39	1.66, 1.66	1.37	1.77, 1.77	2.99 ($C_\varepsilon H$), 7.48 ($N_\varepsilon H_3$)
Phe13	7.92	4.55	2.85, 2.85			6.37 ($C_{2,6}H$), 7.03 ($C_{3,5}H$), 7.03 (C_4H)
Leu14	8.68	4.31	1.53, 1.72	1.34	0.89, 1.02	
Glu15	8.28	4.10	1.96, 2.00	2.52, 2.59		
Glu16	8.95	3.87	1.93, 1.93	2.40, 2.45		
Gly17	8.58	3.37, 4.30				
Thr18	7.62	4.12	4.28	1.07		
Ile19	8.91	4.09	1.74	1.05	0.89, 0.89 ($C_\gamma H_3$)	
Cys20	8.76	4.94	2.88, 3.09			
Asn21	9.74	4.38	2.70, 3.02			6.92, 7.58 ($N_\gamma H_2$)
Met22	8.43	4.46	2.45, 2.45	1.92, 2.03		2.62 ($C_\varepsilon H_3$)
Ala23	8.14	4.28	1.32			
Arg24	8.28	4.29	1.76, 1.85	1.62	3.18, 3.18	7.22 ($N_\varepsilon H$)
Gly25	8.42	3.81, 4.01				
Asp26	8.30	4.67	2.84, 2.84			
Asp27	8.22	4.67	3.66, 3.66			
Met28	7.95	4.50	2.45, 2.55	1.91, 2.04		2.88 ($C_\varepsilon H_3$)
Asp29	8.27	4.71	2.51, 2.68			
Asp30	8.02	4.94	2.39, 2.90			
Tyr31	8.41	5.20	2.59, 2.65			6.93 ($C_{2,6}H$), 6.73 ($C_{3,5}H$)
Cys32	9.45	4.70	2.52, 3.95			
Asn33	9.73	4.94	2.83, 3.31			6.92, 7.68 ($N_\gamma H_2$)
Gly34	8.41	4.18, 4.29				
Lys35	8.58	4.08	1.40	1.68, 1.17	1.49, 1.56	2.91 ($C_\varepsilon H$), 7.46 ($N_\varepsilon H_3$)
Thr36	7.65	4.14	3.72	1.33		
Ala37	8.32	4.13	0.95			
Asp38	8.36	4.63	2.84, 2.93			
Cys39	8.73	5.43	2.64, 2.93			
Pro40		4.30	2.10, 2.20	1.86	3.59, 4.09	
Arg41	8.21	4.18	1.67, 1.73	1.54	3.15	7.19 ($N_\varepsilon H$)
Asn42	8.31	4.92	2.84, 2.84			7.41, 6.85 ($N_\gamma H_2$)
Pro43		4.48	2.20	1.99, 1.85	3.75, 3.82	
His44	8.41	4.63	3.22, 3.26			7.33 (C_2H), 8.58 (C_4H)
Lys45	8.12	4.17	1.69, 1.82	1.37	1.64	2.98 ($C_\varepsilon H$), 7.48 ($N_\varepsilon H_3$)

acids. In preliminary studies, the toxin appears to resemble some vasoactive peptides or neurotoxins. Recently several groups have reported multiple functions for this toxin. Respiratory failure was shown to be the primary cause of death from the toxin in mice, yet rats were rather resistant to waglerin I.[43-45] The toxin (10 μg/mL) does not alter the amplitude of sodium and potassium currents at the nerve endings; however, it causes a decrease in the calcium current.[46,47] The toxin acts at both pre- and post-synaptic neuromuscular junctions of the mouse motor endplate, and

its presynaptic effect is shown to be more potent than the postsynaptic one. The detailed mechanism for the toxic action of waglerins has not yet been fully elucidated. According to a previous report,[42] the intramolecular disulfide bond in this toxic peptide was essential for its biological activity. In our previous study,[48] we have applied NMR analysis and dynamic simulated annealing to derive a three-dimensional structure for waglerin I, one of the two main lethal peptides from this arboreal snake. We further prepared several synthetic analogues of waglerin by replacement of various basic amino acids suspected to be involved in the active site with alanine in an endeavour of elucidating the molecular basis underlying its biological activity. In order to investigate the active site of the toxin, seven analogues of waglerin, [Ala^{3}]-waglerin, [Ala^{7}]-waglerin, [Ala^{10}]-waglerin, [Ala^{14}]-waglerin, [Ala^{18}]-waglerin, [Ala^{20}]-waglerin and [Ala^{22}]-waglerin have been synthesized chemically by single replacement of 7 basic amino acid residues (Lys at residues #3 and #20; Arg at residues #7, #18 and #22; His at residues #10 and #14) one by one with Ala.

NMR analysis and computer modeling of waglerin analogues

The tertiary structures of these analogues in solution were simulated based on the structure of waglerin I which had been determined by NMR and computer modeling previously.[48] It is clear and evident that by comparison with waglerin I (Fig. 7), [Ala^{10}]-waglerin analogue has an apparent twist in the disulfide loop due to a single amino acid substitution at this position. By correlation of structures for each analogue with LD_{50} toxicity bioassays, it was found that the [Ala^{10}]-waglerin exhibited no toxicity, leading to the conclusion that the active site of the native toxin seems to reside in the proximity of the disulfide loop, which is spatially close to His^{10}. The tertiary structure of [Ala^{14}]-waglerin generated from simulation and theoretical calculation also showed a twist closely adjacent to the disulfide loop. Furthermore, the closer the disulfide loop is to the basic amino acid in waglerin, the more influential the basic amino acid is on the toxicity of waglerin. On the other hand, the tertiary structures of all other analogues derived from computer-simulated homology modeling did not show significantly different structures to that of waglerin I. (data not shown). Therefore, it is to be concluded that two histidine residues at positions 10 and 14 indeed play significant roles in the toxicity and structural integrity of waglerin I.

Fig. 7. Superimposition of energy-minimized structures of synthetic analogues (green) with the basic waglerin-I (yellow). Noted that only [Ala^{10}]-waglerin and [Ala^{14}]-waglerin show some twist at or near the disulfide loop region when compared with the structure of waglerin-I. All other analogues show essentially similar conformations.

CONCLUSION AND PERSPECTIVES

Understanding of the functional aspects of life phenomena requires knowledge of the chemistry of various biological molecules, *i.e.* the structural details of these macromolecules such as proteins and peptides and their interaction with their biological targets. At the Institute of Biological Chemistry, Academia Sinica, there is a traditional emphasis and strength in the realm of research in protein chemistry. With the recent advance in the DNA recombination and biotechnology, we have been developing a program along the lines of structural biology and protein engineering with the aim of applying various physical methods in the structural analysis of some biologically relevant proteins or peptides and improving their stability and activity through the newer technique of site-directed mutagenesis. Especially noteworthy is the recent development of cloning techniques in the generation of many previously scarce proteins available for detailed physico-chemical analysis regarding their tertiary structures. Moreover, the sequence of such molecules is now generally amenable and easily obtained from a sequencing analysis of their respective clones, but little or nothing is known about their three-dimensional structures. In this regard, we have first explored the potential of applying Raman and NMR methodologies to structural analysis of various venom toxins in order to lay a firm foundation for research programs under the common theme of structural biology and protein engineering.

Snake venoms are rich sources of proteins, some of which are potent toxins. Three structurally defined groups of protein toxins from Taiwan cobra as studied by Raman spectroscopy in this account, *i.e.* phospholipase A_2, cardio-

toxin, and cobrotoxin, have also been extensively pursued by several groups in this country. The high-resolution NMR structure of cobrotoxin[49] was solved by Yu et al. from Tsing Hua University, essentially complementing the previous X-ray crystal structures of similar neurotoxins from different snake species.[50,51] Although the structural information on cobrotoxin provided by our FT-Raman analysis can not match that obtained by high-resolution NMR and X-ray techniques, it still provided some insight into the microenvironment of Tyr and Trp, which is consistent with the results of NMR and X-ray analysis. Recently, in collaboration with J. F. Kuo's group at Emory University, we reported that cobra cardiotoxin and its various isoforms, like other naturally occurring bioactive amphiphilic polypeptides such as mastoparan and melittin, are specific and strong inhibitors of protein kinase C (PKC).[52] Interestingly receptor-specific cobrotoxin of the same venom, in contrast, showed no effect on PKC. In light of the link between PKC inhibition and cardiotoxin regarding implications for the actual cellular target of these small toxin peptides, it should prove useful to find some defined structural differences between these two classes of cobra toxins in order to account for their drastic functional differences. Bhaskaran et al.[53] recently also published the NMR solution structure of one of the cardiotoxin isoforms, *i.e.* cardiotoxin III. Although some structural differences do exist between cardiotoxin and cobrotoxin,[49,53] it remains an issue of debate and intense interest to elucidate the structural basis underlying the different pharmacological properties as exemplified by these two types of cobra toxins with similar tertiary structures based on these NMR studies. It is worth noting that Wu and his associates also from Tsing Hua University have found different membrane-fusion activity associated with different isoforms of cardiotoxins.[54] They used physical methods such as 2D-NMR and circular dichroism coupled with pH-titration on chemical shifts of amide protons of various amino acid residues in cardiotoxin to detect local conformational change associated with the protonation of a critical histidine residue in the loop I of the toxin.[55] Apparently, by the application of these physical techniques, minor conformational changes in toxin can be observed and correlated with biological activity such as the aggregation/fusion activity of sphingomyelin vesicles. Wu's conclusion that diverse membrane targets may be present for different cardiotoxin isoforms needs further clarification. The cDNAs that encode some of these three classes of cobra toxins[56-59] have been isolated and their nucleotide sequences identified. The potential now exists for large-scale expression and tailoring the specificities of several PLA_2 enzymes and the activity/stability of two classes of small toxins via the site-directed mutagenesis.

As regards the application of high-resolution NMR spectroscopy and computer graphic simulation to the determination of solution structures of various small peptides (< 50 amino acid residues), we have, to date, obtained fruitful results on several examples of biologically active polypeptides which include destruxins.[60,61] polymyxin B and their analogues,[62] mastoparan-B,[63] two linear hexapeptides of destruxin derivatives,[64] echistatin analogue,[65] and waglerin.[66] As a general approach, we searched the literature for some peptides or small proteins (of fewer than 100 amino acid residues) with interesting biological functions and then isolated and purified these materials from their natural sources or through cloning or peptide synthesis. Important insights about the structure/activity correlation of these peptides have been revealed through examination of the simulated graphic models derived from NMR data. As high-resolution X-ray structures of these flexible peptides are few at present, the approach of adopting NMR and computer-graphics model building should yield important insights into the structural features responsible for biological activity. What we have accomplished so far is to lay solid foundations for our future investigations of larger biological macromolecules using physical methods such as Raman and NMR spectroscopy, on which we can gradually build with assurance and confidence. Our current interests have also been extended to lens crystallins with molecular size of more than 20 kDa using near-IR FT-Raman spectroscopy[67,68] and 2D-NMR study of the expressed cobra PLA_2 of 119 amino acid residues.[56,57]

ACKNOWLEDGMENT

We thank Academia Sinica and the National Science Council, Taipei, Taiwan for support.

Received January 13, 1997.

Key Words

Two-dimensional nuclear magnetic resonance (2D-NMR); Near-infrared Fourier transform Raman spectroscopy (near-IR FT-Raman); Snake toxins; Phospholipases A_2; Cobrotoxin; Cardiotoxin; Echistatin γ; Waglerin I; Computer graphic simulated modeling; Site-directed mutagenesis; Protein engineering.

REFERENCES

1. Lee, C. Y. in *Advances in Cytopharmacology* (Ceccarelli, B. and Clementi, F., eds.) Vol. 3, pp. 1-16, Raven Press, New York, 1979.
2. Karlsson, E. in *Snake Venoms*, Handbook of Experimental Pharmacology (Lee, C. Y., ed.) Vol. 52, pp. 159-212, Springer, Berlin, 1979.
3. Yu, N.-T.; Jo, B. H.; O'Shea, D. C. *Arch. Biochem. Biophys.* **1973**, *156*, 71-76.
4. Yu, N.-T.; Lin, T. S.; Tu, A. T. *J. Biol. Chem.* **1975**, *250*, 1782-1785.
5. Tu, A. T. in *Raman Spectroscopy in Biology: principles and applications*, pp. 65-116, John Wiley & Sons, New York, 1982.
6. Wüthrich, K. *NMR of Proteins and Nucleic Acids*, John Wiley & Sons, New York, 1986.
7. MacArthur, M. W.; Driscoll, P. C.; Thornton, J. M. *Trends in Biotech.* **1994**, *12*, 149-153.
8. Chiou, S.-H.; Lin, W.-W.; Chang, W.-P. *Int. J. Peptide Protein Res.* **1989**, *34*, 148-152.
9. Yang, C. C.; Yang, H. J.; Huang, J. S. *Biochim. Biophys. Acta* **1969**, *188*, 65-77.
10. Chiou, S.-H.; Lee, B.-S.; Chang, C.-C.; Yu, N.-T. *Biochem. International* **1991**, *25*, 387-395.
11. Chiou, S.-H.; Lee, B.-S.; Yu, N.-T. *Biochem. International* **1992**, *26*, 747-758.
12. Yang, C. C. *J. Biol. Chem.* **1965**, *240*, 1616-1618.
13. Yang, C. C.; Yang, H. J.; Chiu, R. H. C. *Biochim. Biophys. Acta* **1970**, *214*, 355-363.
14. Menez, A.; Bouet, F.; Tamiya, N.; Fromageot, P. *Biochim. Biophys. Acta* **1976**, *453*, 121-132.
15. Hseu, T. H.; Chang, H.; Hwang, D. M.; Yang, C. C. *Biochim. Biophys. Acta* **1978**, *537*, 284-292.
16. Low, B. W.; Preston, H. S.; Sato, A.; Rosen, L. S.; Searl, J. E.; Rudko, A. D.; Richardson, J. S. *Proc. Natl. Acad. Sci. USA* **1976**, *73*, 2991-2994.
17. Tsernoglou, D.; Petsko, G. A. *Proc. Natl. Acad. Sci. USA* **1977**, *74*, 971-974.
18. Takamatsu, T.; Harada, I.; Hayashi, K. *Biochim. Biophys. Acta* **1980**, *622*, 189-200.
19. Kawano, Y.; Laure, C. J.; Giglio, J. R. *Biochim. Biophys. Acta* **1982**, *705*, 20-25.
20. Areas, E. P. G.; Laure, C. J.; Gabilan, N.; Araujo, P. S.; Kawano, Y. *Biochim. Biophys. Acta* **1989**, *997*, 15-26.
21. Frushour, B. G.; Koenig, F. L. *Biopolymers* **1974**, *13*, 455-474.
22. Yu, N.-T.; Liu, C. S.; O'Shea, D. C. *J. Mol. Biol.* **1972**, *70*, 117-132.
23. Chen, M. C.; Lord, R. C. *J. Am. Chem. Soc.* **1974**, *96*, 4750-4752.
24. Yang, C. C.; Chang, C. C.; Hayashi, K.; Suzuki, T.; Ikeda, I.; Hamaguchi, K. *Biochim. Biophys. Acta* **1968**, *168*, 373-376.
25. Sugeta, H.; Go, A.; Miyazawa, T. *Chem. Lett.* **1972**, 83-86.
26. Sugeta, H.; Go, A.; Miyazawa, T. *Bull. Chem. Soc. Japan* **1973**, *46*, 3407-3411.
27. Aird, S. D.; Kaiser, I. I.; Lewis, R. V.; Kruggel, W. *Arch. Biochem. Biophys.* **1986**, *249*, 296-300.
28. White, S. P.; Scott, D. L.; Otwinowski, Z.; Gelb, M. H.; Sigler, P. B. *Science* **1990**, *250*, 1560-1563.
29. Scott, D. L.; Otwinowski, Z.; Gelb, M. H.; Sigler, P. B. *Science* **1990**, *250*, 1563-1566.
30. Ouyang, C.; Huang, T. F. *Biochim. Biophys. Acta* **1983**, *757*, 332-341.
31. Huang, T. F.; Holt, J. C.; Lukasiewicz, H.; Niewiarowski, S. *J. Biol. Chem.* **1987**, *262*, 16157-16163.
32. Dennis, M. S.; Henzel, W. J.; Pitti, R. M.; Lipari, M. T.; Napier, M. A.; Deisher, T. A.; Bunting, S.; Lazarus, R. A. *Proc. Natl. Acad. Sci. USA*. **1990**, *87*, 2471-2475.
33. Gan, Z.-R.; Gould, R. J.; Jacobs, J. W.; Friedman, P. A.; Polokoff, M. A. *J. Biol. Chem.* **1988**, *263*, 19827-19832.
34. Chen, Y. L.; Huang, T.-F.; Chen, S.-W.; Tsai, I.-H. *Biochem. J.* **1994**, *305*, 513-520.
35. Yasuda, T.; Gold, H. K.; Leinbach, R. C.; Yaoita, H.; Fallon, J. T.; Guerrero, L.; Napier, M. A.; Bunting, S.; Collen, D. *Circulation* **1991**, *83*, 1038-1047.
36. Cooke, R. M.; Carter, B. G.; Murray-Rust, P.; Hartshorn, M. J.; Herzyk, P.; Hubbard, R. E. *Protein. Engng.* **1992**, *5*, 473-477.
37. Saudek, V.; Atkinson, R. A.; Pelton, J. T. ***Biochemistry***. **1991**, *30*, 7369-7372.
38. Calvete, J. J.; Wang, Y.; Mann, K.; Shafer, W.; Niewiarowski, S.; Stewart, G. J. *FEBS Lett.* **1992**, *309*, 316-320.
39. Chen, P. Y.; Wu, S. H.; Wang, K. T. *Protein Engng.* **1994**, *7*, 941-944.
40. Leviton, A. E. *Philip. J. Sci.* **1964**, *93*, 251-276.
41. Weinstein, S. A.; Schmidt, J. J.; Bernheimer, A. W.; Smith, L. A. *Toxicon.* **1991**, *29*, 227-236.
42. Schmidt, J. J.; Weinstein, S. A.; Smith, L. A. *Toxicon.* **1992**, *30*, 1027-1036.
43. Tsai, M. C.; Hsieh, W. H.; Smith, L. A.; Lee, C. Y. *Toxicon.* **1995**, *33*, 363-371.
44. Lin, W. W.; Smith, L. A.; Lee, C. Y. *Toxicon.* **1995**, *33*, 111-114.
45. Aiken, S. P.; McArdle, J. J.; Sellin, L. C.; Schmidt, J. J.; Weinstein, S. A. *Pharmacologist.* **1991**, *33*, 186.

46. Aiken, S. P.; Sellin, L. C.; Schmidt, J. J.; Weinstein, S. A.; McArdle, J. J. *Pharmacology and Toxicology* **1992**, *70*, 459-462.
47. McArdle, J. J.; Xiao, Y.-F.; Aiken, S. P.; Sellin, L. C.; Schmidt, J. J.; Weinstein, S. A. *Neuosci. Soc.* **1992**, *18*, 969.
48. Chuang, L. C.; Yu, H. M.; Chen, C.; Huang, T. H.; Wu, S. H.; Wang, K. T. *Biochim. Biophy. Acta* **1996**, *1292*, 145-155.
49. Yu, C.; Bhaskaran, R.; Chuang, L.-C.; Yang, C.-C. *Biochemistry* **1993**, *32*, 2131-2136.
50. Low, B. W.; Preston, H. S.; Sato, A.; Rosen, L. S.; Searl, J. E.; Rudko, A. D.; Richardson, J. S. *Proc. Natl. Acad. Sci. USA* **1976**, *73*, 2991-2994.
51. Corfield, P. W. R.; Lee, T. J.; Low, B. W. *J. Biol. Chem.* **1989**, *264*, 9239-9242.
52. Chiou, S.-H.; Raynor, R. L.; Zheng, B.; Chambers, T. C.; Kuo, J. F. *Biochemistry* **1993**, *32*, 2062-2067.
53. Bhaskaran, R.; Huang, C. C.; Chang, D. K.; Yu, C. *J. Mol. Biol.* **1994**, *235*, 1291-1301.
54. Chien, K.-Y.; Huang, W.-N.; Jean, J.-H.; Wu, W. *J. Biol. Chem.* **1991**, *266*, 3252-3259.
55. Chiang, C.-M.; Chien, K.-Y.; Lin, H.; Lin, J.-F.; Yeh, H.-C.; Ho, P.; Wu, W. *Biochemistry* **1996**, *35*, 9167-9176.
56. Pan, F.-M.; Yeh, M.-S.; Chang, W.-C.; Hung, C.-C.; Chiou, S.-H. *Biochem. Biophys. Res. Commun.* **1994**, *199*, 969-976.
57. Pan, F.-M.; Chang, W.-C.; Chiou, S.-H. *Biochem. Mol. Biol. International* **1994**, *33*, 187-194.
58. Chang, L.-S.; Wu, P.-F.; Lin, J. *Biochem. Biophys. Res. Commun.* **1996**, *219*, 116-121.
59. Kumar, T. K. S.; Yang, P. W.; Lin, S. H.; Wu, C. Y.; Lei, B.; Lo, S. J.; Tu, S.-C.; Yu, C. *Biochem. Biophys. Res. Commun.* **1996**, *219*, 450-456.
60. Chen, H.-C.; Yeh, S.-F.; Ong, G.-T.; Wu, S.-H.; Sun, C.-M.; Chou, C.-K. *J. Nat. Prod.* **1995**, *58*, 527-531.
61. Yeh, S.-F.; Pan, W.; Ong, G.-T.; Chiou, A.-J.; Chuang, C.-C.; Chiou, S.-H.; Wu, S.-H. *Biochem. Biophys. Res. Commun.* **1996**, *229*, 65-72.
62. Liao, S.-Y.; Ong, G.-T.; Wang, K.-T.; Wu, S.-H. *Biochim. Biophys. Acta.* **1995**, *1252*, 312-320.
63. Chuang, C.-C.; Huang, W.-C.; Yu, H.-M.; Wang, K.-T.; Wu, S.-H. *Biochim. Biophys. Acta* **1996**, *1292*, 1-8.
64. Chiou, A.-J.; Ong, G.-T.; Wang, K.-T.; Chiou, S.-H.; Wu, S.-H. *Biochem. Biophys. Res. Commun.* **1996**, *219*, 572-579.
65. Chuang, L.-C.; Chen, P.-Y.; Chen, C.; Huang, T.-H.; Wang, K.-T.; Chiou, S.-H.; Wu, S.-H. *Biochem. Biophys. Res. Commun.* **1996**, *220*, 246-254.
66. Hsiao, Y.-M.; Chuang, C.-C.; Chuang, L.-C.; Yu, H.-M.; Wang, K.-T.; Chiou, S.-H.; Wu, S.-H. *Biochem. Biophys. Res. Commun.* **1996**, *227*, 59-63.
67. Chiou, S.-H.; Chen, W. *Biochem. International* **1992**, *28*, 401-412.
68. Chiou, S.-H.; Yu, C.-W.; Lin, C.-W.; Pan, F.-M.; Lu, S.-F.; Lee, H.-J.; Chang, G.-G. *Biochem. J.* **1995**, *309*, 793-800.